Molecular Neurobiology (2019) 56:3522–3537
https://doi.org/10.1007/s12035-018-1299-y

Silencing of Long Noncoding RNA SOX21-AS1 Relieves Neuronal Oxidative Stress Injury in Mice with Alzheimer's Disease by Upregulating FZD3/5 via the Wnt Signaling Pathway

Lu Zhang[1] · Yu Fang[2] · Xuan Cheng[1] · Ya-Jun Lian[1] · Hong-Liang Xu[1]

Received: 15 April 2018 / Accepted: 2 August 2018 / Published online: 24 August 2018

Abstract

Alzheimer's disease (AD) represents a progressive neurodegenerative disorder characterized by distinctive neuropathological changes. Recently, long noncoding RNAs (lncRNAs) have become a key area of interest due to their potential in AD therapy. Hence, the aim of the current study was to investigate the effect of lncRNA SOX21-AS1 on neuronal oxidative stress injury in mice with AD via the Wnt signaling pathway by targeting FZD3/5. Microarray analysis was performed to screen AD-related differentially expressed genes (DEGs). Following verification of the target relationship between SOX21-AS1 and FZD3/5, the contents of OH^-, malondialdehyde (MDA), superoxide dismutase (SOD), catalase (CAT), and glutathione peroxidase (GSH-Px) were determined, with the expressions of SOX21-AS1, FZD3/5, β-catenin, cyclin D1, and 4-HNE in hippocampal neuron cells subsequently detected. Cell cycle distribution and apoptosis were evaluated. Bioinformatics analysis revealed that SOX21-AS1 was upregulated in AD, while highlighting the co-expression of SOX21-AS1 and FZD3/5 genes and their involvement in the Wnt signaling pathway. AD mice exhibited diminished memory and learning ability, increased rates of MDA, OH^-, SOX21-AS1, 4-HNE, and elevated levels of hippocampal neuron cell apoptosis, accompanied by decreased levels of SOD, CAT, GSH-Px, FZD3/5, β-catenin, and cyclin D1. Silencing of SOX21-AS1 resulted in decreased OH^-, MDA contents, SOX21-AS1, and 4-HNE, and increased SOD, CAT, GSH-Px, FZD3/5, β-catenin, and cyclin D1, as well as reduced apoptosis of hippocampal neuron cells. Taken together, the key findings of the present study demonstrated that silencing of lncRNA SOX21-AS1 could act to alleviate neuronal oxidative stress and suppress neuronal apoptosis in AD mice through the upregulation of FZD3/5 and subsequent activation of the Wnt signaling pathway.

Keywords Alzheimer's disease · Long noncoding RNA SOX21-AS1 · FZD3/5 · Wnt signaling pathway · Oxidative stress

Introduction

Alzheimer's disease (AD) represents a common irreversible and progressive set of neurodegenerative disorders, which are largely characterized by personality changes and memory loss that ultimately results in dementia [1]. The major histopathological hallmarks of AD include the formation of senile plaques (SP) that arise as a consequence of extracellular deposition of amyloid β-protein (Aβ) and intracellular neurofibrillary tangles (NFTs) composed of the tau protein, as well as the progressively diminished capacity and number of synapses and neurons [2]. Based on current literature, the formations of NFTs and senile plaques are widely thought to be lesions of AD, which is believed to produce neurotoxic effects and facilitate neuronal death through the induction of oxidative stress and inflammation [3, 4]. The risk factors associated with the incidence of AD include age, traumatic brain injury, cerebral stroke, low social activity, poor mental performance, low education level, social exclusion, and physical inactivity [5]. In 2006, statistically speaking, the global prevalence of AD was 26.6 million, with estimations projecting that by 2050, this number would quadruple, which would mean that, one out of 85 people would in the future suffer from the condition [6]. Despite continued efforts in the form of clinical trials, as well as new drug applications for AD treatment, there is still a distinct scarcity in the knowledge of biomarkers that

✉ Lu Zhang
zhangluzl18@163.com

[1] Department of Neurology, The First Affiliated Hospital of Zhengzhou University, No. 1, Jianshe East Road, Erqi District, Zhengzhou 450052, Henan Province, People's Republic of China

[2] ICU, The First Affiliated Hospital of Zhengzhou University, Zhengzhou 450052, People's Republic of China

may help diagnose the disease and offer more effective therapies to alleviate the oxidative stress-induced neuronal injury caused by AD.

Long noncoding RNAs (lncRNAs) can be defined as genomic transcriptions longer than 200 nucleotides (nt) that lack the function of protein coding due to the absence of an open reading frame of significant length [7]. As a regulatory molecule, lncRNAs are a crucial element and play a vital role in a large array of cellular processes through their interaction with some key protein components in the gene regulatory system, highlighting their potential as novel prognostic markers and therapeutic targets in the pathology of AD [8, 9]. SOX21-AS1 is a recently discovered lncRNA that has been described as a good independent prognostic biomarker for oral squamous cell carcinoma marked by its low expression [10]. The Wnt signaling pathway is one of the most conservative pathways in the period of evolution, playing key roles in various biological processes, including adult tissue homeostasis and embryonic development. Its processes can be further divided into two categories: the canonical Wnt signaling pathway (Wnt/β-catenin pathway) and the noncanonical Wnt signaling pathway (planar cell polarity and Wnt/calcium signaling pathways) [11]. Frizzled 3/5 (FZD3/5) is a receptor required for the Wnt signaling pathway that is involved in the development of the central nervous system, including structural plasticity and synaptogenesis [12, 13]. Recent literature has indicated the critical role of the Wnt signaling pathway in neurodegenerative disorders such as AD [14], while evidence has been proposed suggesting that activation of the Wnt signaling pathway inhibited by Frizzled receptor could be a useful therapeutic target in the therapy of AD [15]. Hence, the aim of the present study was to investigate the effects of lncRNA SOX21-AS1 on oxidative stress-induced neuronal injury in AD mice via the Wnt signaling pathway by targeting FZD3/5, in an attempt to identify a novel biomarker for enhanced AD treatment.

Material and Methods

Ethics Statement

All animal experimentation was conducted in strict accordance with the Guide for the Care and Use of Laboratory Animal issued by National Institutes of Health.

Bioinformatics Prediction

The GEO database (http://www.ncbi.nlm.nih.gov/geo) was explored followed by downloading the relative AD chip data (GSE4757) and annotated probe files, which were obtained by detection means using Affymetrix Human Genome U95 Version 2 Array. Background correction and normalization of chip data were conducted by using Affy installation package of R software [16]. Next, the linear model-empirical Bayesian statistical method in the Limma installation package in connection with a traditional t-test was applied in order to perform nonspecific filtration for the expression profile data in a bid to screen the differentially expressed lncRNA [17]. Multi Experiment Matrix (MEM, http://biit.cs.ut.ee/mem/) [18] is a web-based tool (provides hundreds of publicly available gene expression datasets of different tissues, diseases, and conditions, arranged by species and microarray platform type) that we used to predict the co-expression genes among the differentially expressed lncRNA. The KEGG Database (http://www.genome.jp/kegg/pathway.html) was conducted to perform enrichment analysis in order to identify the co-expression genes.

Model Establishment

Thirty-six specific pathogen free (SPF) Kunming (KM) mice ($n = 36$, weight 18–25 g, 18 males and 18 females) were recruited for the purposes of the study. All mice were purchased from the Shanghai Institute of Pharmaceutical Industry (Shanghai, China). All mice were housed on laminar flow shelves with SPF at a constant controlled temperature range between 24 and 26 °C, with a controlled humidity of 45–55%. All food and water provided to the mice was sterilized at high temperature. Next, 36 mice were randomly assigned into 3 groups, namely, the sham group ($n = 12$), the AD group ($n = 12$), and the AD + si-SOX21-AS1 group ($n = 12$).

Mice in the AD group were intraperitoneally injected with 6 ml/kg 1%phenobarbital sodium, and fixed on an operating table after anesthesia had been administered, with the head of the mice fixed using a stereotaxic instrument. Mice hair was cut and disinfected on the roof of skull, while the subcutaneous fascia was peeled in order to expose the parietal bone using a sterile means. Small holes were drilled on both sides of the coronal suture, followed by the injection into the hippocampus region (in reference to the stereotaxic atlas of the mouse): 3 mm in the behind of fonticulus anterior, 2.7 mm below the dura mater, and 2.0 mm outside the midline. A total of 1 μl of $A\beta_{1-40}$ (Sigma-Aldrich Chemical Company, St Louis MO, USA) with micro aggregated peptide was injected at each side. Before injection, 0.1% trifluoroacetic acid (TFA) was used to dilute $A\beta_{1-40}$ to 5 μg/μl at 37 °C for 1 week. After surgery, the tooth powder was used to seal the skull hole and suture the skin. Penicillin G (100,000 units/kg) was intramuscularly injected to mice every day over a 3-day period in order to prevent infection [19]. The mice in the sham group were injected with an equal amount of normal saline. Both the operation and injection methods were sustained in the same manner as conducted in the AD group. The mice in the AD + si-SOX21-AS1 group were injected with $A\beta_{1-40}$ and si-SOX21-

AS1 at the same time, the operation and injection methods were maintained in the same manner as the AD group.

Step-Down Test

Twenty-eight days after the mice had been injected with $A\beta_{1-40}$ on their cella lateralises, the step-down test was initiated on the mice. The box employed in the step-down test was 15 × 15 × 25 cm (length × width × height) in size, with a small platform placed on the bottom of the box, which was the power grid. During the experiment, the mice were initially placed on the platform, from which the mice would jump off and subsequently explore the box. When the mice had jumped off, they would get electric shock, and would then jump back onto the platform to evade nociceptive stimulus. Most of the mice would jump off the platform time and again and then jump back to the platform after receiving an electric shock. The observation index was the total number of errors of experimental mice in a certain period of time after a 24-h period of training.

Object Recognition Test

On the 31st day post AD model establishment, the object recognition test was conducted. The experiment was divided into 3 phases. During the first phase, there was no object in the box and the experimental mice were permitted to freely explore and adapt to the environment over a 5-min period. In the second phase, two identical objects were placed on the same side of the box, and the time the experimental mice used to explore the two objects within 5 min was recorded. In the third phase, a new object was planted in place of the previous objects placed in the second phase, and the time the experimental mice used to explore the two objects within 5 min was recorded in connection with the application of the discrimination index (the time of exploring new object/total time of exploring × 100%) calculated.

Morris Water Maze (MWM) Test

A MWM test was performed on the 33rd day after the establishment of the model of AD mice. The water maze diameter was 150 cm and the pool wall height was 50 cm as well as a water depth of 40 cm with the temperature ranging between 21 and 23 °C. A 10 cm diameter escape platform was placed in the center of the target quadrant, which was 1 cm beneath the water surface. After an adaptive training period, the orientation navigation experiment was conducted as follows: the mice were gently lowered tail-first into the pool facing the wall and the time required to find the platform was recorded. In the event that the mice were located within 120 s, the escape latency time was recorded. If the mice were not located within 120 s and required guidance to the platform and stayed for 20 s, the escape latency time was recorded as 120 s. A spatial probe test was subsequently conducted as follows: the platform was removed after the orientation navigation experiment, with time of residence at the target quadrant recorded.

Transmission Electron Microscope

After the MWM test, the mice were sacrificed, and the hippocampi of 4 mice were placed in 4% glutaraldehyde (prepared by 0.2 M phosphate buffer saline [PBS], pH 7.2) and stored in a refrigerator at 4 °C for later experimentation. The tissues were then washed 3–4 times with 0.1 M PBS times (30 min each time), and then fixed for 2 h. The tissues then underwent an additional wash with 0.1 M PBS 3–4 times (30 min for each), dehydrated with gradient acetone of 30, 50, 70, and 90% respectively for a period of 15 min each, with 100% acetone used twice for a period of 30 min. The tissues were penetrated by anhydrous acetone and epoxy resin, permeated using pure epoxy resin overnight, embedded, and polymerized. Semi thin sections were then prepared for location observation, followed by the preparation of ultrathin sections using LKB-V ultra-microtome. Double staining was performed using both 3% uranyl acetate and lead citrate, after which the tissue sections were observed by means of TEM (Hitachi High-Technologies Corporation, Tokyo, Japan).

Determination of OH^-, MDA, SOD, CAT, and GSH-Px Levels

After the MWM test, the mice were sacrificed. The hippocampi of 4 mice were obtained and treated with homogenate. The levels of OH^-, malondialdehyde (MDA), superoxide dismutase (SOD), catalase (CAT), and glutathione peroxidase (GSH-Px) in the homogenates of the obtained mouse hippocampus were then measured using an OH^- test kit, MDA test kit, SOD test kit, CAT test kit, and GSH-Px test kit purchased from Nanjing Jiangcheng Bioengineering Institute (Nanjing, China). The experiment was conducted in accordance with the instructions of the kit. The parallel experiment was repeated three times.

In Situ Hybridization

Paraffin sections of the mice brain tissues were obtained using conventional xylene dewaxing and gradient alcohol dehydration methods. The expression levels of SOX21-AS1 in the mice hippocampi were evaluated using a situ hybridization kit (Wuhan Boster Biological Technology Co., Ltd., Wuhan, China) while the probe was synthesized by Shanghai Invitrogen Biotechnology Co., Ltd. (Shanghai, China). The tissues were incubated with a mixture of 30% H_2O_2 with distilled water (diluted at 1:10) at room temperature for 10 min for inactivation of the endogenous enzyme and

washed 3 times with distilled water. Pepsin diluted by 3% citric acid was then added to the tissues, mixed, and digested at 37 °C for 30 min. The tissues were then fixed with 1% paraformaldehyde (pH 7.2–7.6) composed of diethy pyrocarbonate (DEPC) at room temperature for 10 min and washed 3 times with distilled water. A pre-hybridization experiment was carried out as follows: firstly, 20 ml of 20% glycerin was added to the bottom of the hybrid box followed by the addition of 20 μl of pre-hybridization liquid to each section at a temperature ranging between 38 and 41 °C for 6 h, followed by the removal of excess liquid. The hybridization experiment was performed as follows: 20 μl of hybridization liquid was added to each section and covered overnight with a protective film at a temperature ranging between 38 and 41 °C. The following day, closed liquid was added to the sections followed by incubation at 37 °C for 30 min, with the excess liquid removed. Next, biotinylated mouse anti-digoxin was added to the sections at 37 °C for 60 min, washed 4 times with PBS (5 min each time), added with streptavidin-biotin complex (SABC) (1:300) at 37 °C for 20 min, and washed with PBS 3 times (5 min each time). The sections were then added with biotinylated peroxidase at 37 °C for 20 min, washed 4 times with PBS (5 min each time), developed by 3, 3′-diaminobenzidine (DAB), and stained by hematoxylin. After full washing, sections were dehydrated by alcohol, cleared by xylene, and mounted. The expression of SOX2-AS1 was measured using an automatic medical color imaging analysis system (Qianping, China) for staining intensity evaluation by semi quantitative means. Four visual fields were selected from each section and the number of positive cells was measured to calculate the mean value.

Immunohistochemistry

The paraffin sections of the mouse brain tissues were obtained and the slides were then placed in a 60 °C incubator for 1 h. The slides were dewaxed and hydrated with xylene I and xylene II for 30 min, respectively, and dehydrated by gradient alcohol. The slides were then placed in a beaker containing diluted potassium citrate solution, followed by performance of microwave antigen retrieval at 90 °C for 10 min. The slides were then permitted to cool at room temperature and washed 3 times with PBS (5 min each time). The tissues were then added with 3% H_2O_2 to inactivate endogenous peroxidase at room temperature for 10 min and blocked by 5% goat serum (Beijing Solarbio Science & Technology Co. ltd., Beijing, China) at room temperature for 20 min. After removal of the sealing liquid, the sections were added with rabbit anti-Aβ monoclonal antibody (1:500, ab2539), rabbit anti-FZD3 polyclonal antibody (1:200, ab217032), rabbit anti-FZD5 polyclonal antibody (1:150, ab75234), rabbit anti-β-catenin polyclonal antibody (1:200, ab32572), rabbit anti-cyclin D1 monoclonal antibody (1:200, ab134175), and rabbit anti-4-hydroxynonenal (4-HNE) polyclonal antibody (1:200, ab46545) incubated overnight at 4 °C and washed three times using PBS (5 min each time). All aforementioned antibodies were purchased from Abcam Inc. (Cambridge, UK) and added in a respective manner until the sections were completely covered. The secondary antibody working solution goat anti-rabbit (ZSGB-BIO, Beijing, China) was then added to the sections and incubated at 37 °C for 1 h, followed by 3 PBS washes (5 min each time). The sections were then developed using DAB (ZSGB-BIO, Beijing, China) for 3–5 min and fully washed under running water. Multifunctional true color cell imaging analysis and management system (Media Cybernetics, Silver Spring, MD, USA) were applied for assessment purposes. Four slices were taken from each specimen and 3 visual fields were randomly selected. Four sections were selected form each sample and 3 visual fields were randomly selected from each section. The number of positive cells was counted under a light microscope, and the mean value was obtained and considered to be a reflection of the expressions of FZD3/5, β-catenin, cyclin D1 and 4-HNE proteins.

Terminal Deoxynucleotidyl Transferase (TdT) -Mediated (dUTP) Nick End-Labeling (TUNEL) Staining

A TUNEL kit (Beyotime Biotechnology Co., Shanghai, China) was employed to observe the apoptosis of the hippocampal neuron cells. The paraffin sections of the hippocampal brain tissue were dewaxed with conventional xylene and rehydrated with gradient alcohol. The paraffin sections were then subsequently soaked in 3% H_2O_2 solution at room temperature for 10 min, washed with PBS for 5 min followed by the addition of 50 μl of protease K (Sigma-Aldrich Chemical Company, St Louis MO, USA) (20 μg/ml) at room temperature for 20 min with the tissue proteins removed accordingly. Next, the paraffin sections were washed 3 times with PBS (5 min each time), added with citrate for antigen retrieval over a 30-min period, and washed twice with PBS (5 min each time). The paraffin sections were added with 50 μl terminal deoxynucleotidyl transferase (TdT) enzyme reaction liquid and stored at 37 °C for 1 h under conditions void of light, followed by 3 PBS washes (5 min each time). The reaction liquid free of TdT enzyme was employed as the negative control. Next, 50 μl anti-digoxigenin labeled by peroxidase was added to the paraffin sections and reacted at 37 °C for 30 min under conditions void of light, washed 3 times with PBS (5 min each time), and developed by DAB (ZSGB-BIO, Beijing, China) for 10 min. The paraffin sections were washed 3 times with PBS, re-stained with hematoxylin, and subsequently observed and photographed under a microscope (Nikon, Tokyo, Japan). Three visual fields were randomly selected to calculate the number of positive cells, followed

by determination of the mean value which was representative of hippocampal neuron cell apoptosis.

Isolation and Culture of Mouse Hippocampal Neuron Cells

The mice were sacrificed followed by the prompt removal of their brains and placed in sterile PBS solution. The hippocampus and cerebral cortex were isolated immediately. After rinsing twice with Hank solution (Thermo Fisher Scientific Inc., Waltham, MA, USA), the tissues were then cut into 0.5~1 mm^3 and added with 0.125% trypsin-ethylenediaminetetraacetic acid (trypsin-EDTA) digestive juice for digestion at 37 °C for 5 min, followed by the addition of DMEM solution to terminate the digestion process. The cells were then seeded into a 35-mm medium with polylysine with the cell density of 1~5 × 10^5 cells/ml, incubated in a 5% CO_2 incubator at 37 °C for 24 h and then incubated with DMEM solution. After 3 days, cytosine arabinoside (Sino-american, Chian) was added to inhibit the growth of the glial cells. After 24 h, they were cultured in DMEM solution and after 3~5 days, the primary hippocampal neuron cells from the mice were obtained.

Dual-Luciferase Reporter Gene Assay

The HEK-293 T cells (ATCC, Manassas, VA, USA) were seeded in the 96-well plates and transfected on the next day when cell density was determined to have reached 80%. The 3′-untranslated region (UTR) wild-type (WT) and mutant (MUT) fragments of FZD3 and FZD5 genes were respectively inserted into luciferase reporter vector psiCheck-2-Control (Promega Corp., Madison, Wisconsin, USA) to construct the psiCheck-2-FZD3-MUT, psiCheck-2-FZD3-WT, psiCheck-2-FZD5-MUT, and psiCheck-2-FZD5-WT plasmids, which were then transfected into the HEK-293T cells with SOX21-AS1vector as well as the negative control plasmid. After transfection for 48 h, a dual-luciferase reporter assay was applied to analyze the luciferase activity in the cell extracts according to the following: 100 μl LAR II and 20 μl cell lysate were added to a measuring tube in order to evaluate the target fluorescence followed by the addition of 100 μl Stop & Glo reagent to evaluate the internal fluorescence. The ratio of target fluorescence to internal fluorescence was calculated as the relative luciferase activity, while the value of fluorescence was evaluated using a fluorescence detector (Promega Corp., Madison, Wisconsin, USA).

Cell Grouping and Transfection

The siRNA sequence of SOX21-AS1 and FZD3/5 genes, the full-length sequence of SOX21-AS1, and the meaningless sequence of the negative sequence were designed. The pcDNA™3.1 plasmid was used to construct SOX21-AS1 and presented with ampicyl resistance (Promega Corp., Madison, Wisconsin, USA). The recombinant plasmids were synthesized by Shanghai GenePharma Co., Ltd. The hippocampal neuron cells of mice in the sham and AD groups were extracted. The hippocampal neuron cells of mice in the AD group were transfected and assigned into 8 groups: the sham group (without treatment), the AD group (without treatment), the negative control (NC) group (transfected with NC plasmid), the si-SOX21-AS1 group (transfected with SOX21-AS1 RNAi plasmid), the SOX21-AS1 vector group (transfected with SOX21-AS1 overexpression plasmid), the si-FZD3 group (transfected with FZD3RNAi plasmid), the si-FZD5 group (transfected with FZD5RNAi plasmid), and the si-SOX21-AS1 + si-FZD3 + si-FZD5 group (co-transfected with SOX21-AS1 and si-FZD3/5 RNAi plasmids). The cells were treated with 0.25% trypsin and suspended using DMEM medium containing 10% FBS at a cell density of 5 × 10^5 cells/ml. The cells were then seeded into 6-well plates and transfected when the cell growth was deemed to have reached 80%. Next, 200 μl serum-free Opti-MEM medium (Gibco Company, Grand Island, NY, USA) was used to dilute 6 μl lipofectamine 2000 (Invitrogen Inc., Carlsbad, CA, USA) and mixed at room temperature for 10 min, with 100 μl serum-free Opti-MEM medium used to dilute 2 μg of the target plasmid which was then mixed at room temperature for 10 min. The above two mixtures were mixed respectively and placed at room temperature for 20 min. The primary culture solution in the 6-well plates was removed and 180 μl Opti-MEM medium was then added into each well. The transfection complex was added into the corresponding cell culture well. Following incubation at 37 °C over a period of 18 h in a 5% CO_2 incubator, the cells were incubated with DMEM complete medium. After incubating for 48 h, the cells were collected for subsequent experimentation.

Reverse Transcription Quantitative Polymerase Chain Reaction

Total RNA was exacted using Trizol (Invitrogen Inc., Carlsbad, CA, USA). After the RNA concentration had been determined using Nanodrop 2000 (Thermo Fisher Scientific Inc., Waltham, MA, USA), 1 μg total RNA was reversely transcribed into cDNA based on the instructions of PrimeScript™ RT reagent kit with gDNA Eraser (Takara Holdings Inc., Kyoto, Japan) by adding with 5 g DNA Eraser Buffer and gDNA Eraser at 42 °C for 2 min in order to eliminate the reaction, at 37 °C for 15 min, and at 85 °C for 5 s. The SYBR® *Premix Ex* Taq™ (Tli RNaseH Plus) kit (Takara Holdings Inc., Kyoto, Japan) was applied in order to perform the RT-qPCR experiment using ABI7500 RT-qPCR instrument (Thermo Fisher Scientific Inc., Waltham, MA, USA) with the reaction conditions employed as follows: predenaturation at 95 °C for 10 min, and 40 cycles of denaturation at 95 °C for 15 s followed by annealing at 60 °C for 30 s.

β-actin was regarded as the internal reference, while the $2^{-\Delta\Delta Ct}$ was used to express the ratio of target genes in the experiment group to the control group. The formula applied was as follows: $\Delta\Delta CT = \Delta Ct_{\text{the experiment group}} - \Delta Ct_{\text{the control group}}$, in which $\Delta Ct = Ct_{\text{target gene}} - Ct_{\beta\text{-actin}}$ [20]. Ct was considered to be the number of amplified cycles when the real-time fluorescence intensity of the reaction reached the set threshold, and the amplification was at the logarithmic growth stage at this point. The primers used in the reaction are depicted in Table 1, which were provided by Shanghai GenePharma Co., Ltd. (Shanghai, China). The parallel experiments were repeated three times.

Western Blot Analysis

The total proteins of the mouse brain tissues were obtained, with the protein concentrations measured in accordance with the instructions of bicinchoninic acid (BCA) kit (Thermo Fisher Scientific Inc., Waltham, MA, USA). A total of 30 μg total proteins were selected for polyacrylamide gel electrophoresis (PAGE) at constant voltage 80 v for 35 min and then at 120 v for 45 min. After electrophoresis, the total proteins were transferred to a polyvinylidene fluoride (PVDF) membrane (Amersham, USA). Membrane blockade was conducted using 5% skimmed milk powder at room temperature for 1 h followed by removal of the sealing solution. The membrane was then added with anti-rabbit FZD3 polyclonal antibody (1:1000, ab217032, Abcam, Cambridge, UK), anti-rabbit FZD5 polyclonal antibody (1:1000, ab14475, Abcam, Cambridge, UK), anti-rabbit β-catenin monoclonal antibody (1:5000, ab32572, Abcam, Cambridge, UK), anti-rabbit cyclin D1 monoclonal antibody (1:10000, ab134175, Abcam, Cambridge, UK), anti-rabbit 4-HNE polyclonal antibody (1:1000, ab46545, Abcam, Cambridge, UK), and anti-mouse β-actin monoclonal antibody (1:5000, ab8225 Abcam, Cambridge, UK) and incubated at 4 °C overnight. Next, the membrane was washed with PBS containing 0.1% Tween-20 (PBST) 3 times (10 min each time), added with the secondary antibody goat anti-mouse or goat anti-rabbit labeled by horseradish peroxidase (1:10000, Jackson, USA) and incubated at room temperature for 1 h, after which PBST was used to wash the membrane 3 times (10 min each time). The samples were then developed using an optical luminescence instrument (GE, USA). Grayscale scanning of the protein bands was conducted using the Image Pro Plus 6.0 software (Media Cybernetics, USA) to analyze the relative expression of proteins. The parallel experiments were repeated three times.

Table 1 The primer sequences for RT-qPCRGene

		Primer sequence
FZD3	F:	5′- ATGGCTGTGAGCTGGATTGTC -3′
	R:	5′- GGCACATCCTCAAGGTTATAGGT -3′
FZD5	F:	5′- GGTGTGCCAGGAAATCACG -3′
	R:	5′- CACAAGCGGCCAGAATTGG -3′
β-catenin	F:	5′-ATCACTGAGCCTGCCATCTG-3′
	R:	5′-GTFGCCACGCCTTCATTCC-3′
cyclin D1	F:	5′ATGGAAGGACCCTTGAGGC-3′
	R:	5′- GCGTTTTCGATAGTCTCTGTGGT-3′
SOX21-AS1	F:	5′-AGCTACGGAGGAAGAGGGTT-3′
	R:	5′-TCAGCAGCGCATGTAAGTGA-3′
HSP86	F:	5′- CATCAATCTCATTCCCAGCA -3′
	R:	5′- TCAGCAACCAAATAGGCAGA-3′
HO-1	F:	5′- CGTGCTCGAATGAACACTCT -3′
	R:	5′-GGAAGCTGAGAGTGAGGACC-3′
GST-1	F:	5′- ATGGCTGTGAGCTGGATTGTC -3′
	R:	5′- GGCACATCCTCAAGGTTATAGGT -3′
β-actin	F:	5′-CGGGACCTGACCGACTACTACCT-3′
	R:	5′-GGCCGTGATCTCCTTCTGC-3′

F forward, *R* reverse, *FZD* frizzled, *LncSOX21-AS1* long noncoding RNA SOX21-AS1, *RT-qPCR* reverse transcription quantitative polymerase chain reaction

Flow Cytometry

After a 48-h transfection process, the culture medium was removed and the cells were washed once again with PBS. The cells were detached with 0.25% trypsin, collected in the flow tube and centrifuged at 179*g* for 5 min with the supernatant discard. The cell concentration was adjusted to 10^6 cells/ml. The cells of each group were then divided into two separate tubes, with the cells in one of the tubes resuspended using 500 μl binding buffer, added with 5 μl Annexin-V-fluorescein isothiocyanate (Annexin-V-FITC) and 5 μl propidium iodide (PI, Sigma, Aldrich, USA), mixed and incubated at room temperature for 15 min under dark conditions. The cell apoptosis of each group within 1 h was evaluated by flow cytometry means. The cells in the other tube were fixed with 70% precooled ethanol for 30 min, centrifuged with supernatant discarded, washed once with cool PBS, added with 100 μl RNase A on water bath at 37 °C for 30 min, added with 400 μl PI dye, and incubated at 4 °C for 30 min under dark conditions. Flow cytometry (BD, USA) was performed to evaluate the cell cycle in each group. The parallel experiments were repeated three times.

Statistical Analysis

All experimental data were statistically analyzed using SPSS 21.0 software (IBM Corp., Armonk, NY, USA). Measurement data were expressed as mean ± standard deviation (SD), the differences between two groups were analyzed by means of *t*-test, and statistical analysis among multiple groups was conducted using one-way analysis of variance (ANOVA). $p < 0.05$ was considered to be statistically significant.

Results

SOX21-AS1 Affects the Neuronal Oxidative Stress Injury in AD Through the Wnt Pathway by Targeting FZD3/5

Microarray analysis was conducted in order to screen the AD-related DEGs. The data analysis of the AD chip GSE4757 revealed that SOX21-AS1 was highly expressed in AD (Fig. 1a), while the co-expression of SOX21-AS1 and FZD3/5 genes and their involvement in the Wnt signaling pathway were found on MEM website (Fig. 1b). Thus, it was confirmed that SOX21-AS1 is expressed highly in AD and was found to target FZD3/5 and mediate the Wnt pathway.

Silencing of SOX21 Increases Learning and Memory Abilities in AD Mice

A step-down test was initially conducted, while the object recognition test, as well as the MWM test, was performed to investigate the learning and memory abilities of the mice. The results of the step-down test as illustrated in Fig. 2a demonstrated that when compared with the sham group, the number of errors made by the mice in the AD and AD + si-SOX21-AS1 groups was significantly increased ($p < 0.05$), while the number of errors made by the mice in the AD + si-SOX21-AS1 was found to be less than that of the AD group ($p < 0.05$). The results of the object recognition test as depicted in Fig. 2b revealed that when compared with the sham group, the mice discrimination indexes in the AD and AD + si-SOX21-AS1 groups were significantly decreased ($p < 0.05$), while the discrimination index of mice in the AD + si-SOX21-AS1 group was higher when compared with that of the AD group ($p < 0.05$). As shown in Fig. 2c, the escape latency time of mice in the AD and AD + Si-SOX21-AS1 groups was longer than that of the sham group ($p < 0.05$), while the escape latency time of mice in the AD + si-SOX21-AS1 group was shorter than that of the AD group ($p < 0.05$). The time of residence at the target quadrant of mice in the AD and AD + si-SOX21-AS1 groups was shorter than that of the sham group ($p < 0.05$), while the time of residence in the target quadrant of mice in the AD + si-SOX21-AS1 group was longer than that of the AD group ($p < 0.05$). Based on the above results, we subsequently concluded that silencing of SOX21-AS1 could enhance the learning and memory abilities of mice with AD.

Silencing of SOX21 Alleviates the Lesions in Hippocampus Tissues of Mice in AD

The hippocampus tissue ultrastructure among the mice in the three groups was observed under a TEM. As shown in Fig. 3, in the sham group, the bodies of mouse hippocampal neuron cells were observed to be complete, with a round nucleus free of wrinkles in the nuclear membrane with clear nuclear pores. Abundant euchromatin was visible in the nucleus and nucleolus could be occasionally observed. An assortment of mitochondria, ribosomes and lysosomes was detected in the cytoplasm free of lipofuscin granules, myelinated and unmyelinated nerve fibers, with the astrocytes found to have normal morphology. In the AD group, the nucleus of hippocampal neuron cells was found to be fragmented, with slight wrinkles in the nuclear membrane with vague nuclear pores. Heterochromatin margination was seen in the nucleus. Various organelles had disintegrated in the cytoplasm with mitochondrial break ridge, cavitation, increased lipofuscin

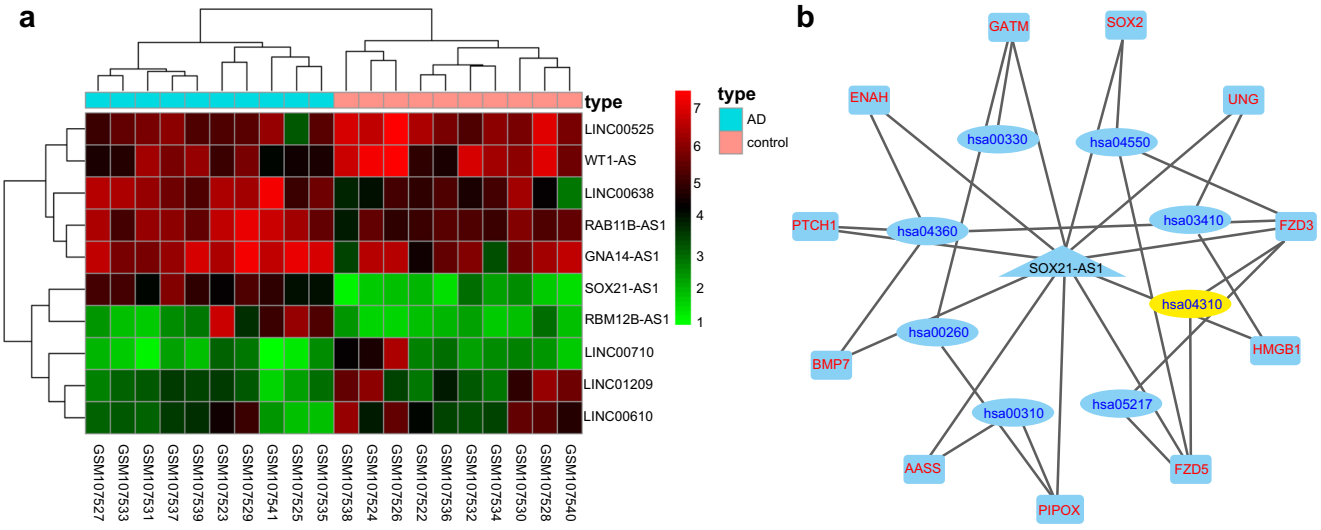

Fig. 1 SOX21-AS1 may target FZD3/5 gene to mediate Wnt signaling pathway and participate in oxidative stress injury in AD mice. **a** Expression of SOX21-AS1 in AD chip GSE4757; **b** Co-expression of SOX21-AS1 and FZD3/5 genes, and hsa04310: Wnt signaling pathway. FZD, frizzled; AD, Alzheimer's disease

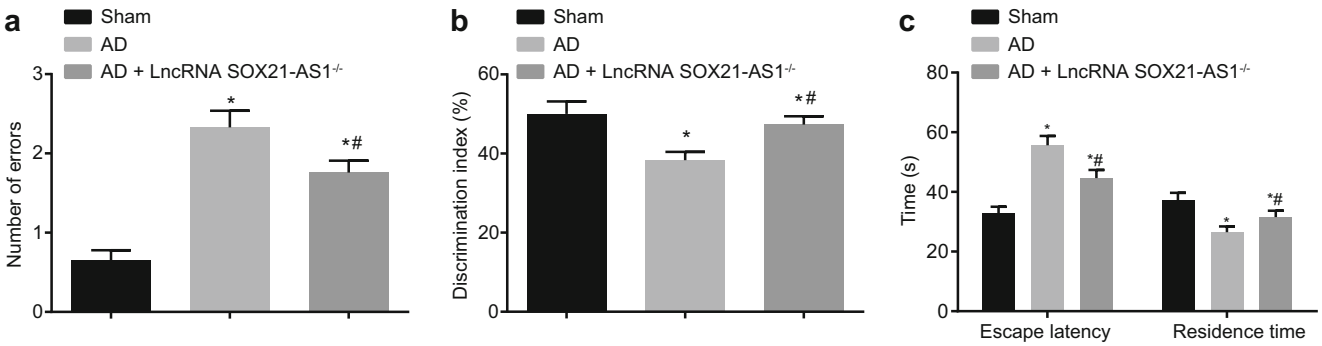

Fig. 2 Silencing of SOX21 increases learning and memory abilities in AD mice. **a** The number of errors of mice in each group; **b** The discrimination index of mice in each group; **c** The escape latency time of mice in each group. *, $p < 0.05$ compared with the sham group; #, $p < 0.05$ compared with the AD group; AD, Alzheimer's disease

granules, and enlarged perinuclear space. In the AD + Si-SOX21-AS1 group, the bodies of mouse hippocampal neuron cells were moderately complete; the nucleus of the hippocampal neuron cells was round and wrinkle free in the nuclear membrane, in addition to the formation of nuclear pores. Abundant heterochromatin margination was seen in the nucleus. Various organelles were observed within the cytoplasm and lipofuscin granules were seen occasionally with small and scattered chromatin. Myelinated and unmyelinated nerve fibers and astrocytes were normal in morphology. The perinuclear space was found to be roughly normal. All the obtained data suggested that silenced SOX21-AS1 could alleviate the lesions of the hippocampus tissues in AD mice, in addition to providing verification indicating that the model had been successfully established.

Silencing SOX21-AS1 Decreases Oxidative Stress Level

MTT assay was conducted in order determine the contents of OH-, MDA, SOD, CAT, and GSH-Px in the mouse hippocampus tissue. As illustrated in Fig. 4, in comparison to the sham group, the AD and AD + si-SOX21-AS1 groups all exhibited increased contents of OH^-, MDA, as well as decreased SOD, CAT, and GSH-Px content (all $p < 0.05$). In comparison to the AD group, the AD + si-SOX21-AS1 group exhibited reduced OH^- and MDA content, while elevated SOD, CAT, and GSH-Px content was detected (all $p < 0.05$). These results demonstrated that the silencing of lncRNA SOX21-AS1 could decrease the contents of OH- and MDA, and increase the contents of SOD, CAT, and GSH-Px.

Silencing SOX21-AS1 Increases the Expression of FZD3/5 and Aβ

Next, in situ hybridization and western blot analysis were performed in order to determine the expressions of SOX21-AS1, FZD3/5, β-catenin, cyclin D1, and 4-HNE in the cells. As shown in Fig. 5a, the cytoplasm of SOX21-AS1 positive cells was deeply stained with blue granular hybridized reaction product. FZD3 protein was found to be predominately expressed within the cytoplasm and cell membrane, while FZD5 protein was mainly expressed in the cytoplasm. The β-catenin protein was positively expressed in the cell membrane and cytoplasm, while cyclin D1 protein in the cytoplasm

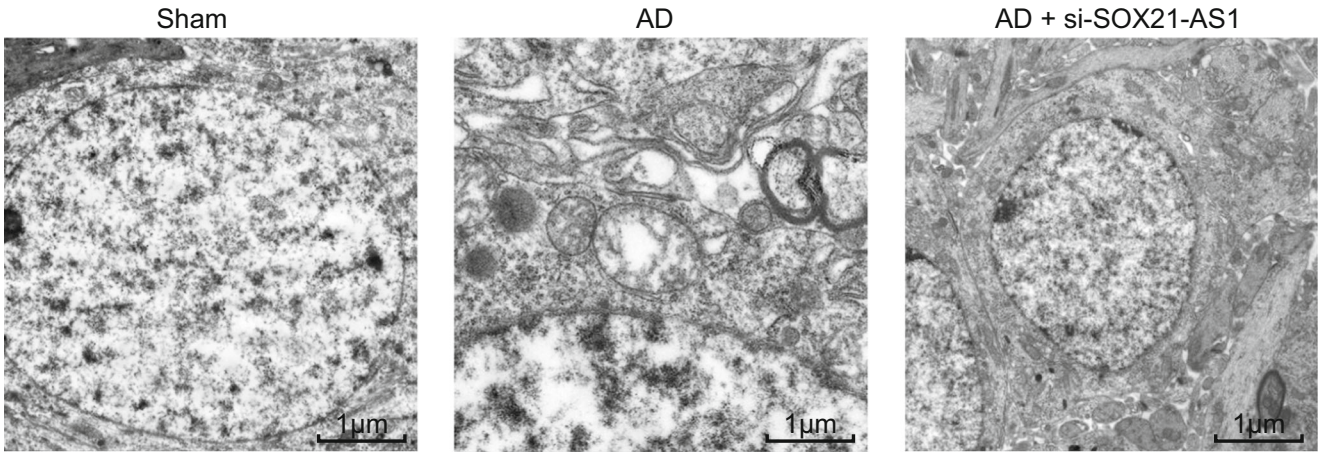

Fig. 3 Silencing of SOX21 alleviates the lesions in hippocampus tissues of mice in AD (8000 ×). **a** Hippocampus tissue ultrastructure of mice in the sham group; **b** Hippocampus tissue ultrastructure of mice in the AD group; **c** Hippocampus tissue ultrastructure of mice in the AD + si-SOX21-AS1 group; AD, Alzheimer's disease

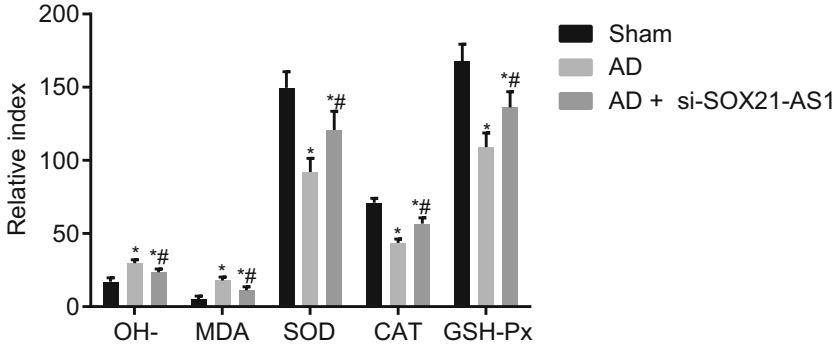

Fig. 4 Silencing of SOX21-AS1 decreases oxidative stress in hippocampus tissue. *, $p < 0.05$ compared with the sham group; #, $p < 0.05$ compared with the AD group; AD, Alzheimer's disease; MDA, malondialdehyde; SOD, superoxide dismutase; CAT, catalase; GSH-Px, glutathione peroxidase

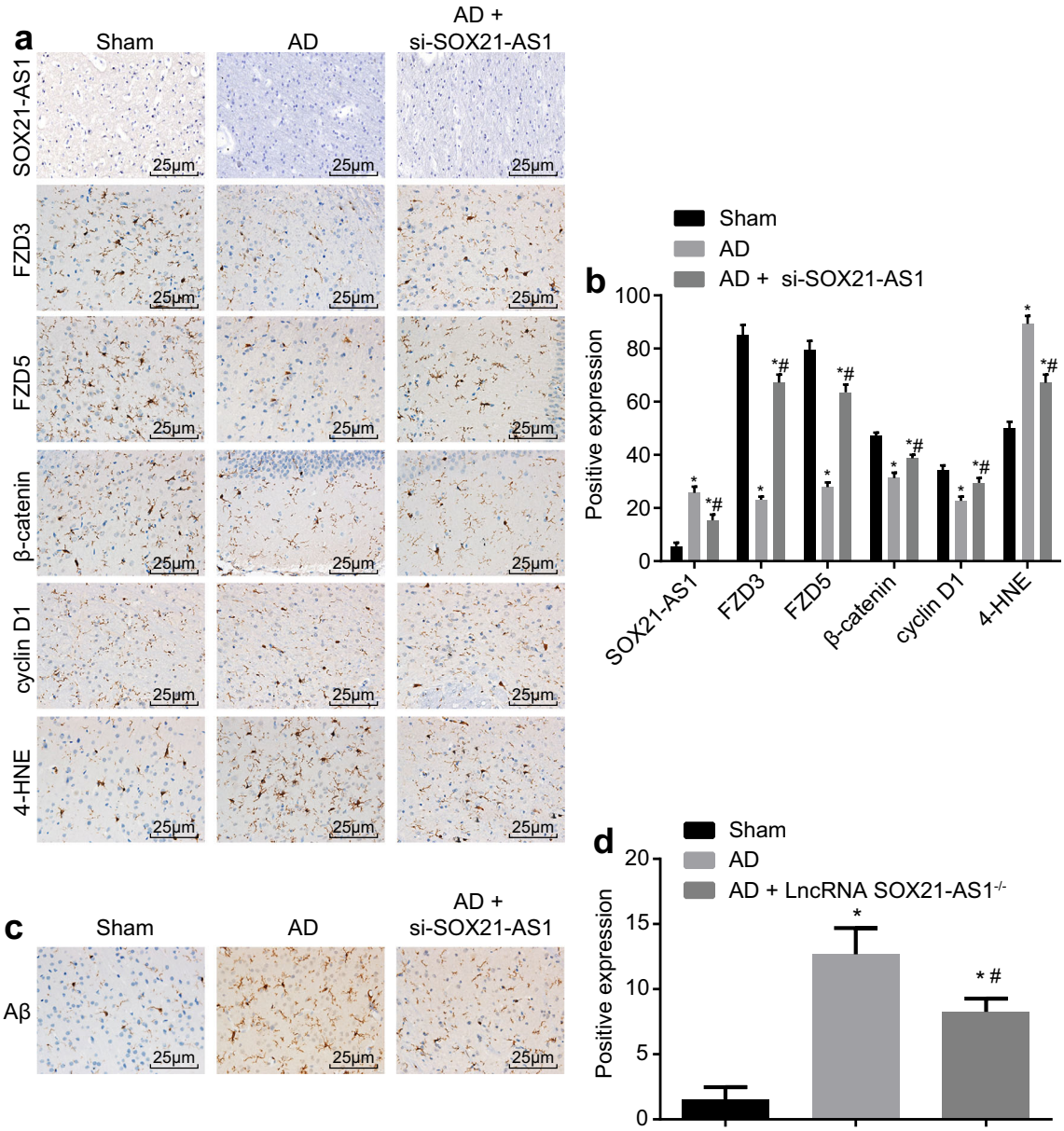

Fig. 5 Silencing SOX21-AS1 increases the expression of FZD3/5. **a** SOX21-AS1 expression in mouse hippocampus tissues measured by in situ hybridization and FZD3/5, β-catenin, cyclin D1, and 4-HNE expressions in mouse hippocampus measured by immunohistochemistry; **b** Positive expressions of SOX21-AS1, FZD3/5, β-catenin, cyclin D1, and 4-HNE in hippocampus tissues; **c** The expression of Aβ in mouse hippocampus tissues measured by immunohistochemistry; **d** Positive expression of Aβ in hippocampus tissues. *, $p < 0.05$ compared with the sham group; #, $p < 0.05$ compared with the AD group; AD, Alzheimer's disease; FZD, frizzled

and nucleus and 4-HNE were considered to be positively expressed when the cytoplasm had been clearly stained. As depicted in Fig. 5b, compared with the sham group, the AD and AD + si-SOX21-AS1 groups exhibited descended expressions of FZD3/5, β-catenin, and cyclin D1 of hippocampus tissue in mice, however increased expressions of SOX21-AS1, 4-HNE, and Aβ (all $p < 0.05$). Compared with the AD group, the AD and AD + si-SOX21-AS1 groups recorded increases in their expressions of FZD3/5, β-catenin, and cyclin D1 of hippocampus tissue in mice, but decreased the expressions of SOX21-AS1 and 4-HNE (all $p < 0.05$). These results indicated that silenced SOX21-AS1 increased the expression of FZD3/5, β-catenin, and cyclin D1 but decreased that of 4-HNE and Aβ in the hippocampus tissue of mice with AD.

Silencing of lncRNA SOX21-AS1 Inhibits Apoptosis of Hippocampal Neuron Cells of AD Mice

In an attempt to investigate the effect of lncRNA SOX21-AS1 on the apoptosis of hippocampal neuron cells in mice, a TUNEL assay was performed. As shown in Fig. 6, compared with the sham group, the AD and AD + si-SOX21-AS1 groups displayed increased mouse hippocampal neuron cell apoptosis (all $p < 0.05$). Compared with the AD group, the AD + si-SOX21-AS1 group exhibited decreased hippocampal neuron cell apoptosis (all $p < 0.05$). Taken together, the obtained data suggested that silencing of lncRNA SOX21-AS1 could suppress the apoptosis of hippocampal neuron cells in mice with AD.

FZD3/5 Are the Target Genes of lncSOX21-AS1

The online analysis software results indicated that there was a potential binding region for SOX21-AS1 and FZD3/5 3'UTR (Fig. 7a). As demonstrated in Fig. 7b, the results of the double luciferase reporter gene assay indicated there to be no significant difference between the FZD3-WT + NC group and the FZD3-MUT + NC and FZD3-MUT + SOX21-AS1 vector ($p > 0.05$), while the FZD3-WT + SOX21-AS1 vector group exhibited decreased luciferase activity ($p > 0.05$). There was no significant difference observed between the FZD5-WT + NC group, and the FZD5-MUT + NC group and the FZD5-MUT + SOX21-AS1 vector group ($p > 0.05$), while the FZD5-WT + SOX21-AS1 vector group showed decreased luciferase activity ($p < 0.05$). The aforementioned results revealed that SOX21-AS1 negatively regulated the transcription of FZD3/5 gene.

Silencing of lncRNA SOX21-AS1 Relieves Oxidative Stress in Hippocampal Neuron Cells of AD Mice

During this experiment, investigative emphasis was placed on lncRNA SOX21-AS1 and its ability to influence oxidative stress. As demonstrated in Fig. 8, compared with the sham group, all the other groups displayed significantly increased OH^- and MDA content in hippocampal neuron cells, while significantly decreased contents of SOD, CAT, and GSH-Px were detected (all $p < 0.05$). No significant difference was detected between the AD group and the NC group regarding the content of OH^-, MDA, SOD, CAT, and GSH-Px in the hippocampal neuron cells; while the si-SOX21-AS1 group showed significantly decreased contents of OH^- and MDA in hippocampal neuron cells, but significantly increased SOD, CAT, and GSH-Px. The SOX21-AS1 vector, si-FZD3, and si-FZD5 groups displayed markedly increased OH^- and MDA content in the hippocampal neuron cells, but significantly decreased SOD, CAT, and GSH-Px. No significant difference was observed in the si-SOX21-AS1 + si-FZD3+ si-FZD5 group in relation to the contents of OH^-, MDA, SOD, CAT, and GSH-Px in the hippocampal neuron cells (all $p < 0.05$). Compared with the si-SOX21-AS1 group, the si-SOX21-AS1 + si-FZD3+ si-FZD5 group showed significantly increased contents of OH^- and MDA in the hippocampal neuron cells, however significantly decreased contents of SOD, CAT, and GSH-Px (all $p < 0.05$). The obtained data led us to conclude that silencing lncRNA SOX21-AS1 could relieve oxidative stress in hippocampal neuron cells of mice with AD.

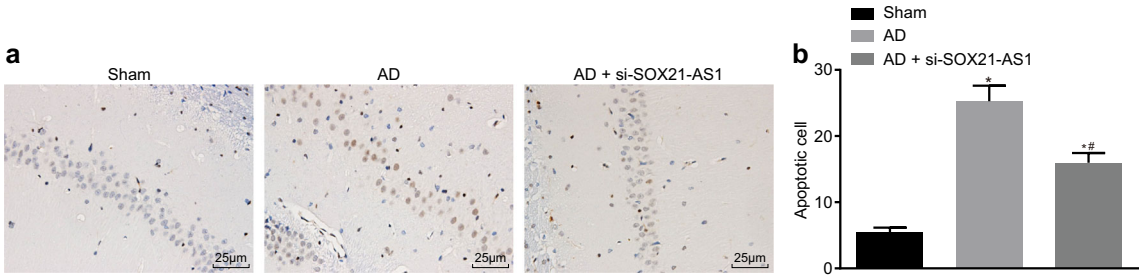

Fig. 6 Apoptosis of hippocampal neuron cells in mice is inhibited after silencing of lncRNA SOX21-AS1. **a** Apoptosis of hippocampal neuron cells in mice among three groups measured by TUNEL staining; **b** Apoptosis rate of hippocampal neuron cells in mice among three groups; *, $p < 0.05$ compared with the sham group; #, $p < 0.05$ compared with the AD group; TUNEL, terminal deoxynucleotidyl transferase (TdT)-mediated (dUTP) nick end-labeling; lncSOX21-AS1, long noncoding RNA SOX21-AS1; AD, Alzheimer's disease

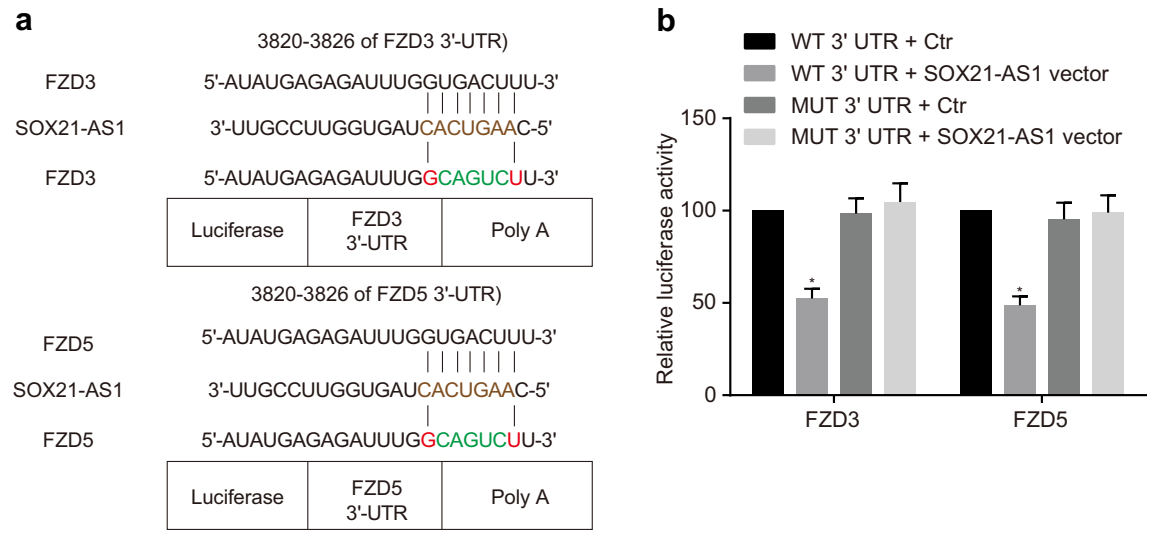

Fig. 7 The targeting relationship between SOX21-AS1 and FZD3/5 genes was identified. **a** Potential binding sites for SOX21-AS and FZD3/5 3'UTR; **b** Double luciferase reporter gene activity; *, $p < 0.05$ compared with the WT + NC group; FZD, frizzled; LncSOX21-AS1, long noncoding RNA SOX21-AS1; NC, negative control; WT, wild type; MUT, mutant type; UTR, untranslated region

Silencing of lncRNA SOX21-AS1 Upregulates FZD3/5 and Activates Wnt Signaling Pathway

In order to acquire an adequate understanding regarding the mechanisms and functions of lncRNA SOX21-AS1 and FZD3/5 on the hippocampal neuron cells of AD mice, their respective expressions were measured in transfected cells in vivo, using RT-qPCR and western blot analysis methods. As shown in Fig. 9, compared with the sham group, all the other groups exhibited significantly decreased FZD3/5, β-catenin and cyclin D1 expressions in the mice hippocampal neuron cells, but significantly increased expressions of SOX21-AS1 and 4-HNE (all $p < 0.05$). Compared with the AD group, no significant differences were detected in the NC group regarding the varying expressions of FZD3/5, β-catenin, cyclin D1, SOX21-AS1, and 4-HNE in the hippocampal neuron cells of the mice (all $p < 0.05$); the si-SOX21-AS1 group displayed notably elevated FZD3/5, β-catenin, and cyclin D1 expressions in the mouse hippocampal neuron cells, while distinctly decreased SOX21-AS1 and 4-HNE expressions were detected. Compared with the AD group, the SOX21-AS1 vector group displayed notably decreased FZD3/5, β-catenin, and cyclin D1 expressions in the mouse hippocampal neuron cells, but significantly increased expressions of SOX21-AS1 and 4-HNE; the si-FZD3 and si-FZD5 groups exhibited significantly descended expressions of FZD3, FZD5, β-catenin, and cyclin D1, but increased 4-HNE expression (all $p < 0.05$); the si-SOX21-AS1 + si-FZD3+ si-FZD5 group showed no significant difference of the expressions of FZD3, FZD5, β-catenin, cyclin D1, and 4-HNE ($p > 0.05$) but decreased expression of SOX21-AS1. Compared with the si-SOX21-AS1 group, the si-SOX21-AS1 + si-FZD3+ si-FZD5 group showed significantly decreased expressions of FZD3/5, β-catenin and cyclin D1, but increased 4-HNE expression (all $p < 0.05$) with no statistical significance observed in relation to the expression of SOX21-AS1 ($p > 0.05$). The results revealed that the silencing of lncRNA SOX21-AS1 could upregulate FZD3/5 and activate the Wnt signaling pathway.

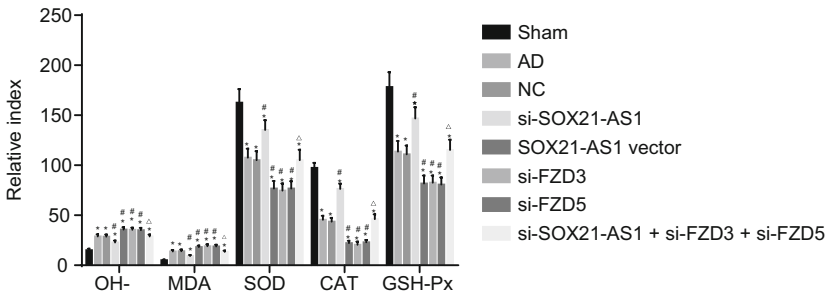

Fig. 8 Silencing of lncRNA SOX21-AS1 relieves oxidative stress in hippocampal neuron cells of AD mice. *, $p < 0.05$ compared with the sham group; #, $p < 0.05$ compared with the AD group; △, $p < 0.05$ compared with the si-SOX21-AS1 group; MDA, malondialdehyde; SOD, superoxide dismutase; CAT, catalase; GSH-Px, glutathione peroxidase; lncSOX21-AS1, long noncoding RNA SOX21-AS1; AD, Alzheimer's disease

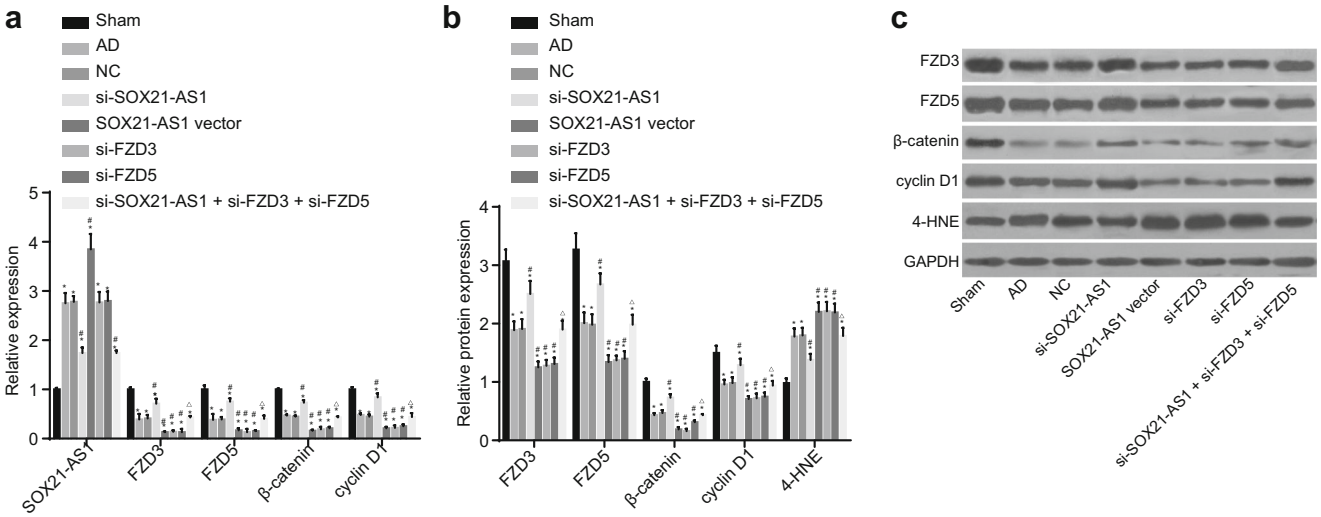

Fig. 9 Silencing of lncRNA SOX21-AS1 upregulates FZD3/5 and activates Wnt signaling pathway. **a** Expressions of SOX21-AS1, FZD3/5, β-catenin, cyclin D1 and 4-HNE in mouse hippocampal neuron cells measured by RT-qPCR; **b**, **c** Protein expressions of SOX21-AS1, FZD3/5, β-catenin, cyclin D1, and 4-HNE in mouse hippocampal neuron cells measured by western blot analysis; *, $p < 0.05$ compared with the sham group; #, $p < 0.05$ compared with the AD group; △, $p < 0.05$ compared with the si-SOX21-AS1 group; RT-qPCR, reverse transcription quantitative polymerase chain reaction; FZD, frizzled; lncSOX21-AS1, long noncoding RNA SOX21-AS1; AD, Alzheimer's disease

Silencing of lncRNA SOX21-AS1 Reduces the mRNA Expression of HO-1, HSP86, and GST

RT-qPCR was conducted in order to examine the mRNA expression of HO-1, HSP86, and GST in the hippocampal neuron cells of the mice. As shown in Fig. 10, compared with the sham group, all other groups displayed markedly increased mRNA expressions of HO-1, HSP86, and GST. There was no significant difference observed in relation to the mRNA expression of HO-1, HSP86, and GST between the AD and NC groups. Compared with the AD group, the si-SOX21-AS1 group exhibited decreased mRNA expression of HO-1, HSP86, and GST in neuron cell ($p < 0.05$) while a contradictory trend was observed in the SOX21-AS1 vector; the si-FZD3 and si-FZD5 groups showed significantly increased mRNA expression of HO-1, HSP86, and GST ($p < 0.05$). No significant differences regarding the mRNA expressions of HO-1, HSP86, and GST were found in the SOX21-AS1 + si-FZD3+ si-FZD5 group compared with the AD group ($p > 0.05$). The results obtained indicated that silencing of SOX21-AS1 decreased the mRNA expression of HO-1, HSP86 and GST in neuron cells of AD mice.

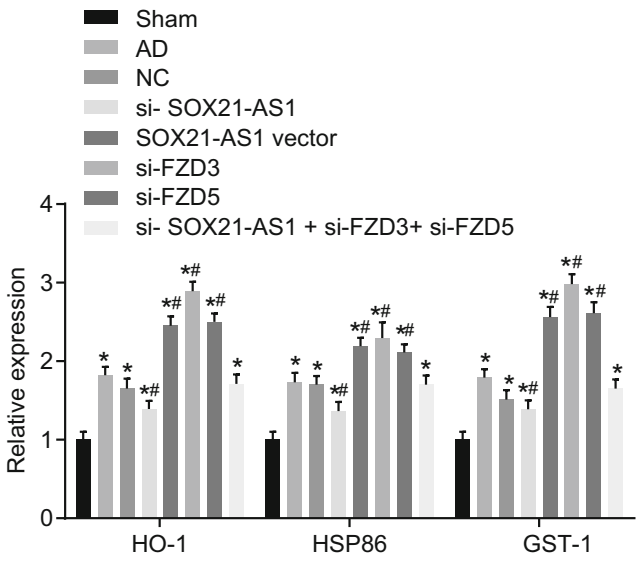

Fig. 10 Silencing of lncRNA SOX21-AS1 reduces the mRNA expression of HO-1, HSP86 and GST. *, $p < 0.05$ compared with the sham group; #, $p < 0.05$ compared with the AD group; AD, Alzheimer's disease; lncSOX21-AS1, long noncoding RNA SOX21-AS1

Silencing of lncRNA SOX21-AS1 Arrests Cells at S Phase and Suppresses Apoptosis of Hippocampal Neuron Cells

Lastly, flow cytometry was employed in order to evaluate the effects of lncRNA SOX21-AS1 on hippocampal neuron cell cycle distribution and apoptosis. As shown in Fig. 11, compared with the sham group, all the other groups displayed significantly elevated cell apoptosis in the hippocampal neuron cells at the G1 phase and decreased cell apoptosis in hippocampal neuron cells at S phase. This indicated that apoptosis was notably increased (all $p < 0.05$). Compared with the AD group, the NC group exhibited no significant difference in cell cycle distribution and apoptosis among the hippocampal neuron cells (all $p < 0.05$), while the si-SOX21-AS1 group showed significantly decreased cell apoptosis in mouse hippocampal neuron cells at the G1 phase and increased cell apoptosis in hippocampal neuron cells at the S phase, indicating that apoptosis was distinctly decreased; the SOX21-AS1 vector, si-FZD3, and si-

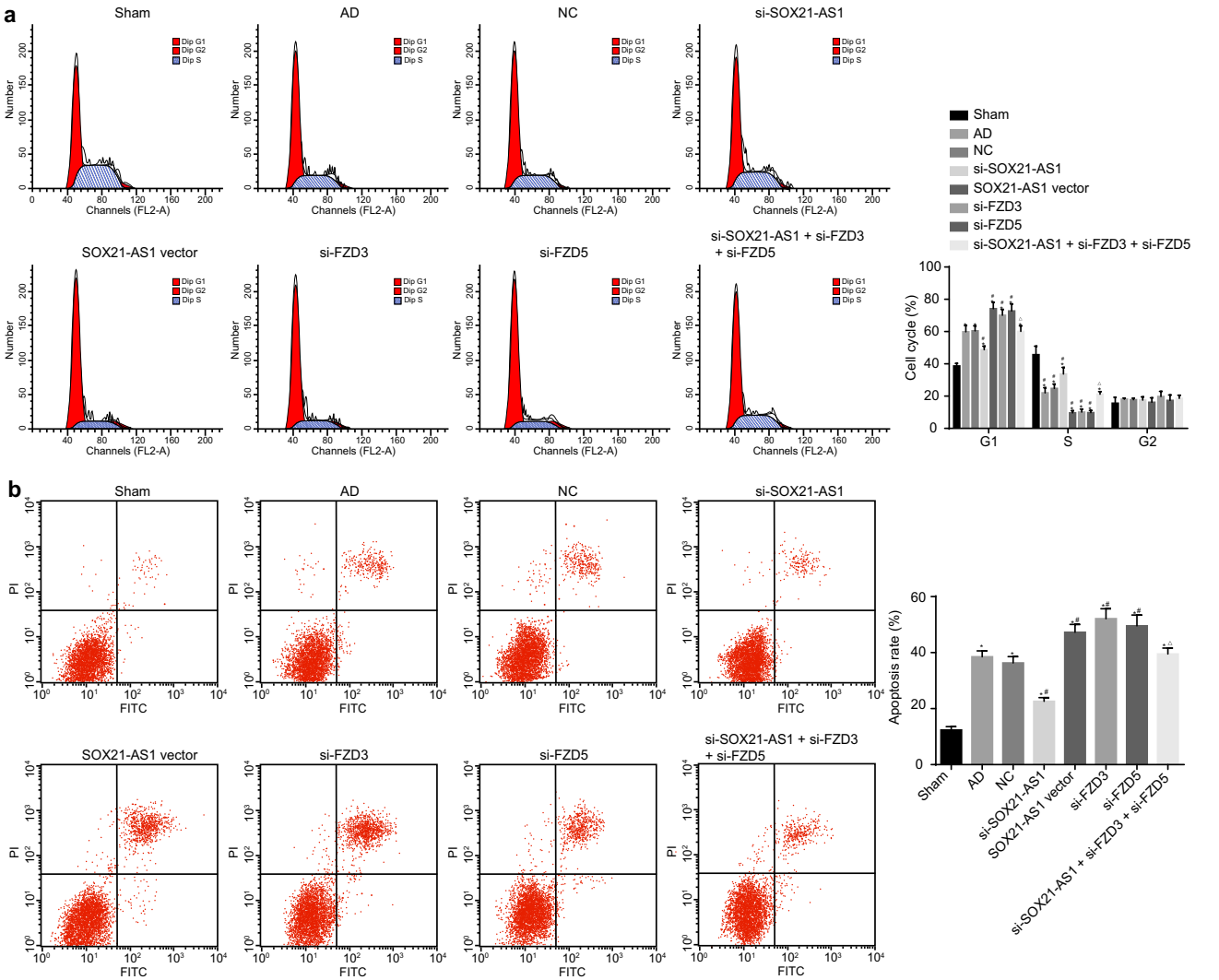

Fig. 11 Silencing of lncRNA SOX21-AS1 arrests cells at S phase and suppresses apoptosis of hippocampal neuron cells. **a** Hippocampal neuron cell cycle distribution determined by flow cytometry; **b** Hippocampal neuron cell apoptosis determined by flow cytometry; *, $p < 0.05$ compared with the sham group; #, $p < 0.05$ compared with the AD group; △, $p < 0.05$ compared with the si-SOX21-AS1 group; FZD, frizzled; lncSOX21-AS1, long noncoding RNA SOX21-AS1

FZD5 groups were noted to have significantly increased cell apoptosis in hippocampal neuron cells at the G1 phase and decreased cell apoptosis in mouse hippocampal neuron cells at the S phase, demonstrating that apoptosis was significantly elevated (all $p < 0.05$); no significant differences were detected among the si-SOX21-AS1 + si-FZD3 + si-FZD5 group in relation to cell cycle distribution and apoptosis in the hippocampal neuron cells of the mice (all $p > 0.05$). Compared with the si-SOX21-AS1, the si-SOX21-AS1 + si-FZD3 + si-FZD5 group showed significantly increased cell apoptosis among the hippocampal neuron cells at the G1 phase and decreased cell apoptosis in hippocampal neuron cells at the S phase, indicating that apoptosis was notably elevated (all $p < 0.05$). All the observed data suggested that silencing of lncRNA SOX21-AS1 could arrest cells at the S phase while inhibiting apoptosis of the hippocampal neuron cells.

Discussion

As one of the most neurodegenerative conditions, AD is a progressive disease characterized by memory loss and cognitive decline. More recently, oxidative stress has been highlighted as a vital determinant in the pathogenesis of AD [21, 22]. Noncoding RNAs have been reported to influence AD by maintaining the balance between healthy stress response and the pathophysiological Aβ cascade [23]. The abnormal expressions of lncRNAs could activate several signaling pathways including the MAPK, ERK, and Wnt/β-catenin pathways [24, 25]. During the current study, AD mice models were successfully established, and the collective results demonstrated that downregulated lncRNA SOX21-AS1 could potentially act to induce the expression of FZD3/5 through activation of the Wnt signaling pathway, ultimately contributing

to the alleviation of neuronal oxidative stress in addition to the inhibition of neuronal apoptosis in AD.

SOX21 represents a high-mobility group box transcription factor that has been reported to be a repressor of neuronal differentiation during the development phase of the nervous system [26]. The relationship between oxidative stress and AD is based on its negative influence on several major pathological processes such as Abeta-induced neurotoxicity and metal dyshomeostasis [27]. Hezroni et al. asserted that the conserved element of linc-SOX21-B is strongly correlated with the conserved brain and neural tube enhancer (VISTA, element hs488) [28]. Similarly, our study demonstrated that lncRNA SOX21-AS1 could promote neuronal oxidative stress in AD; this finding was further supported by the descended MDA, 4-HNE, and ascended SOD, CAT, GSH-Px, β-catenin expressions in the si-SOX21-AS1 group. Importantly, poorly-expressed lncRNA SOX21-AS1 was revealed to alleviate oxidative stress by decreasing the mRNA expressions of HO-1, HSP86, and GST. Declined expressions of MDA and 4-HNE have been reported to confer a protective effect in cases of AD [29]. The expressions of CAT, GSH-Px, and β-actin were previously found to be ascended in brain tissues after donepezil HCl treatment, which has been reported to share an association with decreased learning and memory injury due to AD [30]. Additionally, antioxidant enzymes (SOD and GSH-Px) have been shown to play a significant role on the antioxidant defense system by preventing oxidative injury [31]. What's more, our study demonstrated that lncRNA SOX21-AS1 could inhibit neuronal apoptosis in AD, a finding which is largely consistent with current existing literature. A previous report declared that silencing of SOX21-AS1 in SAS cells could drastically stimulate cell growth, migration, and invasion, ultimately resulting in the inhibition of cell apoptosis [10]. Moreover, a previous study suggested that the downregulation of SOX21 could reduce cell apoptosis in human glioma [32]. Collectively, our results indicated that lncRNA SOX21-AS1 might be an important target for the treatment of AD.

It has been noted that lncRNAs could affect the behaviors of malignant cells by regulating a large array of target genes, and the downstream signaling pathways [33]. In our study, the co-expression patterns between lncRNA SOX21-AS1 and FZD3/5 in AD were investigated. Our findings provided evidence suggesting that FZD3/5, a target gene of lncRNA SOX21-AS1, is negatively regulated by lncRNA SOX21-AS1, indicating that lncRNA SOX21-AS1 associated functions of AD might be associated with FZD3/5. FZD3-deficient embryo has previously been reported to regulate the organization of neuronal projections, independent of enteric neural crest cell migration [34]. A previous report suggested that FZD5 influences the establishment of neuronal polarity, and in the morphogenesis of neuronal processes through the activation of the noncanonical Wnt [35]. Our study also revealed that the overexpression of lncRNA SOX21-AS1 or knockdown of FZD3/5 could act to suppress neuronal apoptosis and promote neuronal oxidative stress, as well as activating the Wnt signaling pathway in AD. Studies have revealed that SOX21, as a gene transcription factor, could affect inheritable alopecia together with the Wnt signaling pathway [36]. Additionally, upregulation of the Wnt receptor FZD3 in addition to activation of the Wnt signaling could result in weakened levels of cell apoptosis in cases of chronic lymphocytic leukemia (CLL) [37]. More importantly, through the activation of Wnt/β-catenin signaling pathway, osthole induced neural stem cells (NSCs) proliferation and neuronal differentiation but reduced apoptosis in AD [38]. Taken together, the results of the present study have presented evidence suggesting that decreased expression of lncRNA SOX21-AS1 could result in the upregulation of FZD3/5, which was accompanied by vast improvements in neuronal oxidative stress and suppressed neuronal apoptosis in AD via the Wnt signaling pathway.

In conclusion, the data obtained and reported in the current study could form the basis shedding light as to how the knockdown of lncRNA SOX21-AS1 may result in alleviation of neuronal oxidative stress and inhibition of neuronal apoptosis in patients with AD by upregulating the expression of FZD3/5 through inhibiting activation of the Wnt signaling pathway. Our findings may provide a further rational for the clinical use of available treatments of AD, which would ultimately result in enhanced patient therapeutics and care. Although our findings have significant implication for therapeutic development in AD treatment, the mechanism by which mediating the interaction between lncRNA SOX21-AS1, FZD3/5, and Wnt in AD still requires further elucidation.

Acknowledgements We would like to acknowledge the helpful comments on this paper received from our reviewers.

Compliance with Ethical Standards

All animal experimentation was conducted in strict accordance with the Guide for the Care and Use of Laboratory Animal issued by National Institutes of Health.

Conflict of Interest The authors declare that they have no conflict of interest.

References

1. Puzzo D, Gulisano W, Palmeri A, Arancio O (2015) Rodent models for Alzheimer's disease drug discovery. Expert Opin Drug Discov 10(7):703–711. https://doi.org/10.1517/17460441.2015.1041913
2. Liu C, Cui G, Zhu M, Kang X, Guo H (2014) Neuroinflammation in Alzheimer's disease: chemokines produced by astrocytes and chemokine receptors. Int J Clin Exp Pathol 7(12):8342–8355
3. Shaw LM, Vanderstichele H, Knapik-Czajka M, Clark CM, Aisen PS, Petersen RC, Blennow K, Soares H et al (2009) Cerebrospinal fluid biomarker signature in Alzheimer's disease neuroimaging

initiative subjects. Ann Neurol 65(4):403–413. https://doi.org/10.1002/ana.21610
4. Scuderi C, Stecca C, Valenza M, Ratano P, Bronzuoli MR, Bartoli S, Steardo L, Pompili E et al (2014) Palmitoylethanolamide controls reactive gliosis and exerts neuroprotective functions in a rat model of Alzheimer's disease. Cell Death Dis 5:e1419. https://doi.org/10.1038/cddis.2014.376
5. Isaev NK, Stelmashook EV, Genrikhs EE, Oborina MV, Kapkaeva MR, Skulachev VP (2015) Alzheimer's disease: an exacerbation of senile phenoptosis. Biochemistry (Mosc) 80(12):1578–1581. https://doi.org/10.1134/S0006297915120056
6. Brookmeyer R, Johnson E, Ziegler-Graham K, Arrighi HM (2007) Forecasting the global burden of Alzheimer's disease. Alzheimers Dement 3(3):186–191. https://doi.org/10.1016/j.jalz.2007.04.381
7. Xiang J, Guo S, Jiang S, Xu Y, Li J, Li L, Xiang J (2016) Silencing of long non-coding RNA MALAT1 promotes apoptosis of glioma cells. J Korean Med Sci 31(5):688–694. https://doi.org/10.3346/jkms.2016.31.5.688
8. Maruyama R, Suzuki H (2012) Long noncoding RNA involvement in cancer. BMB Rep 45(11):604–611
9. Zhang Z (2016) Long non-coding RNAs in Alzheimer's disease. Curr Top Med Chem 16(5):511–519
10. Yang CM, Wang TH, Chen HC, Li SC, Lee MC, Liou HH, Liu PF, Tseng YK et al (2016) Aberrant DNA hypermethylation-silenced SOX21-AS1 gene expression and its clinical importance in oral cancer. Clin Epigenetics 8:129. https://doi.org/10.1186/s13148-016-0291-5
11. Song X, Wang S, Li L (2014) New insights into the regulation of Axin function in canonical Wnt signaling pathway. Protein Cell 5(3):186–193. https://doi.org/10.1007/s13238-014-0019-2
12. Kishimoto M, Ujike H, Okahisa Y, Kotaka T, Takaki M, Kodama M, Inada T, Yamada M et al (2008) The frizzled 3 gene is associated with methamphetamine psychosis in the Japanese population. Behav Brain Funct 4:37. https://doi.org/10.1186/1744-9081-4-37
13. Chen M, Zhong W, Hu Y, Liu J, Cai X (2015) Wnt5a/FZD5/CaMKII signaling pathway mediates the effect of BML-111 on inflammatory reactions in sepsis. Int J Clin Exp Med 8(10):17824–17829
14. Inestrosa NC, Varela-Nallar L, Grabowski CP, Colombres M (2007) Synaptotoxicity in Alzheimer's disease: the Wnt signaling pathway as a molecular target. IUBMB Life 59(4–5):316–321. https://doi.org/10.1080/15216540701242490
15. Inestrosa NC, Toledo EM (2008) The role of Wnt signaling in neuronal dysfunction in Alzheimer's disease. Mol Neurodegener 3:9. https://doi.org/10.1186/1750-1326-3-9
16. Fujita A, Sato JR, Rodrigues Lde O, Ferreira CE, Sogayar MC (2006) Evaluating different methods of microarray data normalization. BMC Bioinformatics 7:469. https://doi.org/10.1186/1471-2105-7-469
17. Smyth GK (2004) Linear models and empirical bayes methods for assessing differential expression in microarray experiments. Stat Appl Genet Mol Biol 3:Article3. https://doi.org/10.2202/1544-6115.1027
18. Adler P, Kolde R, Kull M, Tkachenko A, Peterson H, Reimand J, Vilo J (2009) Mining for coexpression across hundreds of datasets using novel rank aggregation and visualization methods. Genome Biol 10(12):R139. https://doi.org/10.1186/gb-2009-10-12-r139
19. Zhang YY, Yang LQ, Guo LM (2015) Effect of phosphatidylserine on memory in patients and rats with Alzheimer's disease. Genet Mol Res 14(3):9325–9333. https://doi.org/10.4238/2015.August.10.13
20. Livak KJ, Schmittgen TD (2001) Analysis of relative gene expression data using real-time quantitative PCR and the 2(−Delta Delta C(T)) method. Methods 25(4):402–408. https://doi.org/10.1006/meth.2001.1262
21. Xu W, Weissmiller AM, White JA 2nd, Fang F, Wang X, Wu Y, Pearn ML, Zhao X et al (2016) Amyloid precursor protein-mediated endocytic pathway disruption induces axonal dysfunction and neurodegeneration. J Clin Invest 126(5):1815–1833. https://doi.org/10.1172/JCI82409
22. Manolopoulos KN, Klotz LO, Korsten P, Bornstein SR, Barthel A (2010) Linking Alzheimer's disease to insulin resistance: the FoxO response to oxidative stress. Mol Psychiatry 15(11):1046–1052. https://doi.org/10.1038/mp.2010.17
23. Faghihi MA, Modarresi F, Khalil AM, Wood DE, Sahagan BG, Morgan TE, Finch CE, St Laurent G 3rd et al (2008) Expression of a noncoding RNA is elevated in Alzheimer's disease and drives rapid feed-forward regulation of beta-secretase. Nat Med 14(7):723–730. https://doi.org/10.1038/nm1784
24. Li R, Zhang L, Jia L, Duan Y, Li Y, Bao L, Sha N (2014) Long non-coding RNA BANCR promotes proliferation in malignant melanoma by regulating MAPK pathway activation. PLoS One 9(6):e100893. https://doi.org/10.1371/journal.pone.0100893
25. Ma Y, Yang Y, Wang F, Moyer MP, Wei Q, Zhang P, Yang Z, Liu W et al (2016) Long non-coding RNA CCAL regulates colorectal cancer progression by activating Wnt/beta-catenin signalling pathway via suppression of activator protein 2alpha. Gut 65(9):1494–1504. https://doi.org/10.1136/gutjnl-2014-308392
26. Matsuda S, Kuwako K, Okano HJ, Tsutsumi S, Aburatani H, Saga Y, Matsuzaki Y, Akaike A et al (2012) Sox21 promotes hippocampal adult neurogenesis via the transcriptional repression of the Hes5 gene. J Neurosci 32(36):12543–12557. https://doi.org/10.1523/JNEUROSCI.5803-11.2012
27. Zhao Y, Zhao B (2013) Oxidative stress and the pathogenesis of Alzheimer's disease. Oxidative Med Cell Longev 2013:316523. https://doi.org/10.1155/2013/316523
28. Hezroni H, Koppstein D, Schwartz MG, Avrutin A, Bartel DP, Ulitsky I (2015) Principles of long noncoding RNA evolution derived from direct comparison of transcriptomes in 17 species. Cell Rep 11(7):1110–1122. https://doi.org/10.1016/j.celrep.2015.04.023
29. Singh M, Dang TN, Arseneault M, Ramassamy C (2010) Role of by-products of lipid oxidation in Alzheimer's disease brain: a focus on acrolein. J Alzheimers Dis 21(3):741–756. https://doi.org/10.3233/JAD-2010-100405
30. Li Q, Chen M, Liu H, Yang L, Yang G (2012) Expression of APP, BACE1, AChE and ChAT in an AD model in rats and the effect of donepezil hydrochloride treatment. Mol Med Rep 6(6):1450–1454. https://doi.org/10.3892/mmr.2012.1102
31. Qiang H, Liu H, Ling M, Wang K, Zhang C (2015) Early steroid-induced osteonecrosis of rabbit femoral head and Panax notoginseng Saponins: mechanism and protective effects. Evid Based Complement Alternat Med 2015:719370–719310. https://doi.org/10.1155/2015/719370
32. Ferletta M, Caglayan D, Mokvist L, Jiang Y, Kastemar M, Uhrbom L, Westermark B (2011) Forced expression of Sox21 inhibits Sox2 and induces apoptosis in human glioma cells. Int J Cancer 129(1):45–60. https://doi.org/10.1002/ijc.25647
33. Subramanian M, Jones MF, Lal A (2013) Long non-coding RNAs embedded in the Rb and p53 pathways. Cancers (Basel) 5(4):1655–1675. https://doi.org/10.3390/cancers5041655
34. Sasselli V, Boesmans W, Vanden Berghe P, Tissir F, Goffinet AM, Pachnis V (2013) Planar cell polarity genes control the connectivity of enteric neurons. J Clin Invest 123(4):1763–1772. https://doi.org/10.1172/JCI66759
35. Slater PG, Ramirez VT, Gonzalez-Billault C, Varela-Nallar L, Inestrosa NC (2013) Frizzled-5 receptor is involved in neuronal polarity and morphogenesis of hippocampal neurons. PLoS One 8(10):e78892. https://doi.org/10.1371/journal.pone.0078892
36. Ford SJ, Bigliardi PL, Sardella TC, Urich A, Burton NC, Kacprowicz M, Bigliardi M, Olivo M et al (2016) Structural and functional

analysis of intact hair follicles and pilosebaceous units by volumetric multispectral optoacoustic tomography. J Invest Dermatol 136(4): 753–761. https://doi.org/10.1016/j.jid.2015.09.001

37. Zhou XX, Wang X (2013) Role of microRNAs in chronic lymphocytic leukemia (review). Mol Med Rep 8(3):719–725. https://doi.org/10.3892/mmr.2013.1599

38. Yao Y, Gao Z, Liang W, Kong L, Jiao Y, Li S, Tao Z, Yan Y et al (2015) Osthole promotes neuronal differentiation and inhibits apoptosis via Wnt/beta-catenin signaling in an Alzheimer's disease model. Toxicol Appl Pharmacol 289(3):474–481. https://doi.org/10.1016/j.taap.2015.10.013